Research Article

Dan The Pham, Toan Quoc Tran, Luu Van Chinh, Linh Phuong Nguyen, Ton Nu Thuy An, Nguyen Huu Thuan Anh*, Duong Thanh Nguyen*

Anti-tumor effect of liposomes containing extracted Murrayafoline A against liver cancer cells in 2D and 3D cultured models

https://doi.org/10.1515/chem-2022-0122
received October 5, 2021; accepted December 23, 2021

Abstract: Murrayafoline A (MuA) is a natural compound with diverse biological activities, including cytotoxicity against cancer cells, but suffers from poor water solubility and low specificity. In order to improve the potential of MuA as a candidate for cancer treatment, MuA-loaded liposomes were prepared with the liposomal membrane consisting of dioleoylphosphatidylcholine and cholesterol. Dynamic light scattering measurements showed that the MuA-loaded liposomes had a *z*-average particle size of 104.3 ± 6.4 nm (mean ± SD; n = 3) and a polydispersity index of 0.15 ± 0.02 (mean ± SD; n = 3). The encapsulation efficiency was 55.3 ± 2.3% (mean ± SD; n = 3). The *in vitro* cytotoxicity of encapsulated MuA was attenuated at IC_{50} = 21.97 μg/mL compared to 6.24 μg/mL for free MuA, against HepG2. In contrast, MuA-loaded liposomes were significantly more effective at inhibiting cell growth in HepG2 cancer spheroids, which indicated that they were able to reach the interior layers of the microtumor. Taken together, these results showed that the encapsulation of MuA in liposomes is a good research direction to improve this natural compound's potential as a candidate for cancer treatment.

Keywords: Murrayafoline A, liposome, 3D cell culture, cancer spheroid, HepG2

*** Corresponding author: Nguyen Huu Thuan Anh,** Institute of Environmental Technology and Sustainable Development, Nguyen Tat Thanh University, Ho Chi Minh City, Vietnam; Faculty of Food and Environmental Engineering, Nguyen Tat Thanh University, Ho Chi Minh City, Vietnam, e-mail: nhtanh@ntt.edu.vn
*** Corresponding author: Duong Thanh Nguyen,** Graduate University of Science and Technology, 18 Hoang Quoc Viet St., Cau Giay Dist., Hanoi, Vietnam; Institute of Marine Biochemistry, Vietnam Academy of Science and Technology (VAST), 18 Hoang Quoc Viet St., Cau Giay Dist., Hanoi, Vietnam; Institute of Chemistry, Vietnam Academy of Science and Technology (VAST), 18 Hoang Quoc Viet St., Cau Giay Dist., Hanoi, Vietnam, e-mail: ntduong182@gmail.com
Dan The Pham: University of Science and Technology, Department of Life Sciences Hanoi (USTH), 18 Hoang Quoc Viet St., Cau Giay Dist., Hanoi, Vietnam, e-mail: danpt.bi9064@st.usth.edu.vn
Toan Quoc Tran: Institute of Natural Products Chemistry, 18 Hoang Quoc Viet St., Cau Giay Dist., Hanoi, Vietnam; Graduate University of Science and Technology, 18 Hoang Quoc Viet St., Cau Giay Dist., Hanoi, Vietnam, e-mail: tranquoctoan2010@gmail.com
Luu Van Chinh: Institute of Natural Products Chemistry, 18 Hoang Quoc Viet St., Cau Giay Dist., Hanoi, Vietnam, e-mail: chinhluuvan@gmail.com
Linh Phuong Nguyen: Hanoi Medical University, 1 Ton That Tung St., Dong Da Dist., Hanoi, Vietnam, e-mail: nplinh239@gmail.com
Ton Nu Thuy An: Institute of Environmental Technology and Sustainable Development, Nguyen Tat Thanh University, Ho Chi Minh City, Vietnam; Faculty of Food and Environmental Engineering, Nguyen Tat Thanh University, Ho Chi Minh City, Vietnam, e-mail: tntan@ntt.edu.vn

1 Introduction

Cancer is a major cause of health problems and mortality worldwide, with liver cancer being the sixth most common type and the second leading cause of death. The causes of liver cancer include diabetes, chronic hepatitis B virus and hepatitis C virus infection, excessive consumption of alcohol, and smoking tobacco [1]. According to the American Cancer Society, the global death rate (per 100,000 people) for liver cancer has more than doubled from 2.8 to 6.7% (1980–2016), at approximately 700,000 deaths annually [2]. Therefore, continuous research focused on screening, developing, and improving treatments for liver cancer is an important objective.

Historically, plant [3,4] and fungal [5,6] species had provided many promising natural compounds that were eventually developed into anticancer drugs. *Glycosmis stenocarpa* (Drake) Tan is a woody shrub of the *Glycosmis* genus in the family Rutaceae. Members of this genus have been used in traditional medicine to treat a variety of different ailments [7,8]. In 2005, Cuong et al. successfully isolated the carbazole derivative Murrayafoline A (MuA)

from the roots of *G. stenocarpa* (M = 211.259 Da) [9]. This compound has been shown to possess various biological activities [10–12]. Concerning its cytotoxicity, MuA displayed promising results against liver cancer (HepG2), lung cancer (LU-1), prostate cancer (LNCaP), leukemia (HL-60), and epithelial cancer (KB) [11–13]. Test results also showed that free MuA induced a 48.21% decrease in tumor formation density and a 71.33% decrease in the average tumor size compared to the negative control (1% DMSO) [14,15]. However, MuA's poor water solubility ($\log P$ = 2.448) [16,17] hinders the absorption, distribution, and bioavailability of free MuA. Furthermore, normal cells are also susceptible to damage [18,19]. Conventional drug delivery methods (e.g., intravenous infusion used for the poorly soluble Vinca alkaloids) exacerbate this problem. Free MuA would be circulated in the bloodstream without any targeting system, travel through different tissues, and damage healthy cells before reaching the tumor mass [20].

In order to resolve the poor water solubility and low specificity of MuA, liposomal encapsulation is a promising solution. Liposomes are spherically shaped microscopic vesicles consisting of one or more phospholipid bilayer membranes enclosing discrete aqueous spaces [21]. Depending on their physicochemical properties, drug molecules can be encapsulated in either the core or the membrane [21]. Liposomes present several unique advantages, such as improved biocompatibility, bioavailability, and degradability [22,23]. Most importantly, their membranes can be modified with various molecules/macromolecules to control the drug delivery and release process. For example, cholesterol (Chol) improves membrane rigidity and drug retention, polyethylene glycol (PEG) prolongs circulation time, and targeting ligands (e.g., peptides, antibodies, aptamers) increase drug specificity significantly. Currently, some liposomal drugs have been approved by the United States Food and Drug Administration (FDA), such as Myocet (breast cancer), Doxil (ovarian cancer), and Marqibo (acute lymphoblastic leukemia) [24]. Thus, using liposomes for MuA delivery is a viable technique to improve MuA's potential as a candidate chemotherapeutic drug.

In this study, we prepared MuA-loaded liposomes from dioleoylphosphatidylcholine (DOPC) (T_m = −17°C) modified with Chol. The prepared liposome formulations were assessed in terms of particle size, size distribution, and surface charge using dynamic light scattering (DLS). Cytotoxicity was tested using the traditional MTT assay. The anti-tumor activity of MuA-loaded liposomes was tested using a three-dimensional (3D) *in vitro* cell culture model, as it has been demonstrated that cancer cell behavior is reflected more accurately in 3D cultures [25,26].

2 Materials and methods

2.1 Materials

Chol, DOPC, and polycarbonate (PC) membranes (100 nm) were obtained from Avanti Polar Lipids (Alabaster, AL, USA). MuA was extracted and isolated from the roots of *G. stenocarpa*. 3-(4,5-Dimethylthiazol-2-yl)-2,5-diphenyltetrazolium bromide (MTT) was obtained from Thermo Fisher Scientific (Waltham, MA, USA). 4′,6-Diamidino-2-phenylindole, live/dead assay, and Dulbecco's modified Eagle's medium (DMEM) medium were obtained from Invitrogen (Carlsbad, CA, USA). Trypan blue, poly(ethylene glycol) diacrylate average (PEGDA) M_n 700, 2-hydroxy-4′-(2-hydroxyethoxy)-2-methylpropiophenone (PI), and phosphate-buffered saline (PBS) tablets were obtained from Sigma-Aldrich (St. Louis, MO, USA). HepG2 cells were obtained from American Type Culture Collection (ATCC; Manassas, VA, USA). Laboratory-grade chloroform ($CHCl_3$) was obtained from Chemsol (Hochiminh City, Vietnam). High-performance liquid chromatography-grade methanol (MeOH) was obtained from Merck (Kenilworth, NJ, USA). Other reagents were of commercial special grade and were used without any additional purification.

2.2 Extraction of MuA

G. stenocarpa roots were cleaned, dried, and ground into a powder. The root powder (2.5 kg) was macerated in methanol (12.5 L × 3 times). The combined solution was then filtered and concentrated with a rotary evaporator to yield the methanol extract. This concentrate was then partitioned with *n*-hexane, yielding the *n*-hexane fraction. After solvent removal, the condensed *n*-hexane fraction was subjected to silica gel column chromatography with *n*-hexane/ethylacetate [10:1 (v/v)] as the eluant. The eluates were collected in aliquots of 250 mL, with each aliquot representing a fraction. The first 12 fractions were then checked by thin-layer chromatography for the presence of MuA. Then, fractions 5–8 were combined,

concentrated, and redissolved in *n*-hexane/ethylacetate [100:1, (v/v)] to crystallize MuA. This precipitate was then recrystallized for the second time in *n*-hexane/ethylacetate [100:1, (v/v)] to purify MuA. The obtained crystals were dried, powdered, and stored at 4°C. The final yield was approximately 9.5 g of MuA (0.38% dry root weight). The product was elucidated by several spectroscopic methods (infrared spectroscopy [IR], H nuclear magnetic resonance [^{1}H NMR], and mass spectrometry [MS]).

Murrayafoline A (9.5 g): white, monoclinic crystals, $C_{14}H_{13}NO$, m.p. 50–52°C (lit. low melting point [3]). MS (*m*/*z*, % intensity): 211 (M^+, 100), 196 (73), 182 (3), 168 (43), 167 (36), 139 (5), 106 (9), 84 (6). IR ν_{max} (cm^{-1}, KBr disc): 3,448 (N–H), 2,996, 2,942, 2,916, 2,840, 1,924, 1,694, 1,590 (C═C), 1,502, 1,388, 1,332 (C–N), 1,304, 1,278, 1,130, 1,104 (C–O), 1,036, 942, 852, 742, 670. ^{1}H NMR δ_{ppm} (400 MHz, $CDCl_3$): d 8.14 (1H, br, N–H), 8.01 (1H, d, J = 7.32 Hz, H-5), 7.47 (1H, s, H-4), 7.37 (1H, d, J = 8.28 Hz, H-8), 7.20 (1H, t, J = 1.84 Hz, H-7), 7.19 (1H, t, J = 1.84 Hz, H-6), 6.72 (1H, s, H-2), 3.97 (3H, s, O-Me), 2.52 (1H, s, H-9). ^{13}C NMR δ_{ppm} (100 MHz, $CDCl_3$): d 145.3 (C-1), 139.4 (C-8a), 129.4 (C-4a), 127.9 (C-3), 125.5 (C-8), 124.3 (C-5a), 123.5 (C-1a), 120.4 (C-6), 119.1 (C-5), 112.5 (C-4), 110.9 (C-7), 107.6 (C-2), 55.4 (1-OMe), 21.9 (C-9).

2.3 Preparation of MuA-loaded liposomes

Thin-film hydration was used to synthesize liposomes, followed by extrusion to attain the desired particle size. In a 1.5 mL Eppendorf, 250 µL of 0.025 M DOPC, 27.6 µL of 0.01 M Chol, and 109.3 µL of 0.003 M MuA were combined and vortexed for 60 s. Rotary evaporation (30°C, 250 mbar, rotational speed 2) was used to slowly remove the solvent ($CHCl_3$), leaving behind a thin membrane composed of DOPC, Chol, and MuA. Distilled water (4 mL) was added, followed by sonication (40°C, 30 s) to hydrate and peel off the thin film. The resulting suspension was opaque and contained MuA encapsulated in liposomes of varying sizes and unencapsulated MuA. Dialysis was used to remove unencapsulated MuA (MWCO = 14,000 Da, 1 L of dH_2O, 24 h). A mini-extruder (Avanti Polar Lipids, Alabaster, AL, USA) fitted with 100 nm PC membranes was used to restrict the liposomes into specified size ranges and reduce polydispersity. Each sample was extruded for 50 rounds, with each round counted as one passing of the suspension through the PC membrane. Extruded liposomes were stored at 4 or 37°C. The same procedure was used to prepare blank liposomes without the addition of MuA.

2.4 Characterization of MuA-loaded liposomes

The *z*-average, peak size, and polydispersity index (PDI) of the liposome samples stored at 4 and 37°C were monitored for 30 days using a Zetasizer Nano ZS (Malvern, UK). To determine the encapsulation efficiency (EE%) and drug loading content (DL%), water was removed from the samples using rotary evaporation (45°C, 0 mbar, rotational speed 3) until only a dry, thin film was left behind.

To disintegrate the liposomes and release the entrapped MuA, the dried liposome film was dissolved in 3.5 mL of MeOH/$CHCl_3$ [3:1, (v/v)] and sonicated for 2 min. Then, 100 µM of this solution was pipetted from the flask and mixed with 2,900 µM MeOH/$CHCl_3$ [3:1, (v/v)] for 30 s, followed by vortexing. This mixture was then transferred to a clean cuvette, and the sample's absorbance was measured at 243 nm using a Hitachi U-2900 spectrophotometer (Hitachi, Tokyo, Japan) against the MeOH/$CHCl_3$ [3:1, (v/v)] standard. EE% and DL% values were calculated according to the following equations:

$$\text{EE\%} = \frac{\text{The amount of MuA in the liposomes (µmol)}}{\text{The total amount of MuA (µmol)}} \times 100,$$

$$\text{DL\%} = \frac{\text{Mass of MuA in the liposomes (µg)}}{\text{Mass of MuA loaded liposomes (µg)}} \times 100.$$

The MuA-loaded liposomes were monitored at 4 and 37°C over 24 h to assess the storage stability of liposomes. At different time points, aliquots were withdrawn to determine the size and EE%.

Dialysis was used to study the release patterns of MuA-loaded liposomes and free MuA. MuA-loaded liposomes or free MuA (1 mL) were placed in dialysis bags (MWCO = 14,000 Da), with 50 mL of PBS (pH 7.4, 0.01 M) containing Tween 80 (0.5wt%) as the dialysate. The incubation temperature was either 4 or 37°C, with moderate shaking (100 rpm). Aliquots of the dialysis medium (1 mL) were collected at pre-determined time points and replaced with equal volumes of fresh PBS. The total quantity of MuA in the dialysate at each time point was determined using UV-Vis spectrophotometry. Results were averaged from three biological repeats, and presented as mean ± SD.

2.5 Two-dimensional (2D) *in vitro* cytotoxicity assay

2.5.1 Cell culture

Human hepatocellular carcinoma cell line (HepG2) from the ATCC was cultured as a single layer in DMEM, supplemented with 10% fetal bovine serum (Invitrogen, Carlsbad, CA), 100 IU/mL penicillin, and 100 mg/mL streptomycin (Corning Cellgro, Mediatech, Inc., Manassas, VA, USA). Cells were maintained at 37°C in a humidified incubator supplemented with 5% CO_2. Tests were performed on cells at the exponential phase.

2.5.2 *In vitro* cytotoxicity

The MTT assay was used to evaluate the cytotoxicity of free MuA and MuA-loaded liposomes. Cells were seeded at a density of 1×10^4 cells per well in a 96-well plate (Corning Inc., Corning, NY, USA) and incubated for 24 h. Then, growth medium was replaced with MuA-loaded liposomes or free MuA solution at equivalent drug doses ranging from 0.01 to 40 μg/mL. After incubation at specified time intervals, 20 μL of MTT reagent (5 mg/mL) was added to each well and the cells were incubated for another 4 h at 37°C. This was followed by 150 μL of MTT solvent to each well. The plate was wrapped in aluminum foil and agitated on an orbital shaker until formazan had fully dissolved. Within 1 h, the absorbance of each well was measured on a Spark Plate Reader (Tecan, Switzerland) at OD = 590 nm. Untreated HepG2 cells were used as control. Cell viability was determined according to the following equation:

$$\text{Cell viability (\%)} = \frac{A_{\text{sample}} - A_{\text{blank}}}{A_{\text{control}} - A_{\text{blank}}} \times 100.$$

2.6 3D *in vitro* cytotoxicity assay

2.6.1 Cancer spheroid formation

Cancer spheroids were grown as described previously [27]. Briefly, hydrogel-based microwells were prepared from PEGDA using photolithography. PEGDA 98% (M_W = 700 Daltons) and (2-hydroxy-40-(2-hydroxyethoxy)-2-methylpropiophenone) (PI) were dissolved in PBS at concentrations of 20% (v/v) and 0.02% (v/v), respectively. After careful mixing, a drop of this solution was placed on the surface of a glass plate and pressed down by a cover slip to spread into a very thin hydrogel layer. This hydrogel layer was designed to keep cells from interacting with the glass substrate beneath. Photopolymerization (365 nm, 10 s, 16 cm distance) was performed with an Omnicure S2000 lamp (320–500 nm, Ontario, Canada) at 100 mW/cm^2. The hydrogel-coated cover slip was then transferred to a flat plate with spacers (500 μm). Then, 500 μL of the hydrogel solution was added under the cover slip to prepare the second hydrogel layer. A photomask was placed on top of the cover glass, followed by 40 s of UV exposure. The polymerized hydrogels (a square tab of PEGDA with microwells in it) were then rinsed with PBS for a day to remove all residual PEGDA and PI. The stock HepG2 suspension was diluted with DMEM to create a solution with 0.2×10^6 cells/mL. Then, 3 mL of this solution was added to each well containing one hydrogel tab (six-well plate). Once the cell seeding phase was finished, 3 mL of fresh DMEM was added to replace the used medium. HepG2 spheroids were cultured at 37°C in a humidified incubator supplemented with 5% CO_2. The growth medium was changed every 3 days.

2.6.2 *In vitro* anti-tumor activity

To study the effects of MuA-loaded liposomes on 3D cancer spheroids, HepG2 cells were allowed to grow for 1 week after seeding. On day 7, the growth medium was removed and replaced by 2 mL of fresh DMEM. Free MuA, MuA-loaded liposomes, and blank liposomes were dissolved in DMEM to achieve their respective concentrations, and 1 mL of each solution was added to a well, at a total volume of 3 mL for each well in the six-well plate. Cells were then cultured at 37°C, 5% CO_2 for 1 day, with cell viability closely monitored. HepG2 cancer spheroids were then collected and dissociated using 0.25% trypsin–EDTA. Cells were then washed twice with PBS, combined with an equal volume of 0.4% trypan blue, and mixed thoroughly for 3 min to stain. Unstained (viable) and stained (dead) cells were counted on a hemacytometer, and the final value was presented as a percentage of live cells.

2.7 Statistical analysis

All experiments were carried out at least three times, and the quantitative data were presented as mean ± SD. The analysis of variance between at least three groups or

Student's *t*-test between two groups was used to make statistical comparisons. Statistical significance was defined as *P*-values of 0.05 and *P*-values of 0.01.

3 Results and discussion

3.1 Extraction of MuA

MuA was extracted from *G. stenocarpa* roots according to the procedure described in Section 2.2. The final yield was approximately 9.5 g, which accounted for 0.38% of dry root weight. Crystals were white and monoclinic and analyzed as $C_{14}H_{13}NO$. The confirmed structure of MuA agreed well with spectral data as described in ref. [10].

In the IR spectra, the peak at 3,448 cm^{-1} was assigned to the N–H bond. Significant peaks at 2,996, 2,942, 2,916, and 2,840 cm^{-1} were assigned to the stretching of the C–H bond in –CH, $-CH_2$ or $-CH_3$ groups. Strong peaks at 1,590 cm^{-1} indicated the existence of C=C bonds, whereas peaks at 1,502, 1,450, and 1,388 cm^{-1} indicated the presence of aromatic ring absorptions. The substituted benzene ring is represented by three peaks at 942, 852, and 742 cm^{-1}. Meanwhile, a molecular ion peak at *m*/*z* 211 and a base peak at *m*/*z* 196 were revealed in EI-MS analysis.

In the ^1H NMR spectra, a H-bonded methoxyl group was found at d 3.97. Two doublets ascribed to H-5 at d 8.01 and H-8 at 7.37 suggested ortho-substitution of ring A. H-6 and H-7 were responsible for two more pairs of triplets at d 7.19 and 7.20, respectively. Additionally, ^1H NMR spectra revealed one methyl group (H-9-Me) at d 2.52. At d 7.47, the other aromatic proton, H-4, emerged as a singlet.

^{13}C NMR and DEPT spectra indicated the presence of 12 carbons in the structure of the product compound. They consisted of quaternary carbons, aromatic carbons, one methyl group, and one methoxyl carbon. At 145.27 and 139.39 ppm, the methoxyl proton resonating at d 3.97, displayed cross peaks with C-1 and C-8a. Aromatic carbon displayed absorption peaks between 107 and 129 ppm, whereas geminal methyl carbon displayed a peak at 21.89 ppm. Further confirmation of the structure is shown in Table 1.

Table 1: NMR spectral data for MuA

Position	δ^1H	$\delta^{13}C$	DEPT
1	—	145.3	C
1a	—	123.5	C
2	6.72, s	107.6	CH
3	—	127.9	C
4	7.47, s	112.5	CH
4a	—	129.4	C
5	8.01, d	119.1	CH
5a	—	124.3	C
6	7.19, t	120.4	CH
7	7.20, t	110.9	CH
8	7.37, t	125.5	CH
8a	—	139.4	C
9-Me	2.52, s	21.9	CH_3
N–H	8.14	—	—
1-OMe	3.97, s	55.4	CH_3

3.2 Characterization of blank liposomes

Liposomes were synthesized with DOPC as the base phospholipid and Chol as a stabilizer. To survey their stability, different DOPC/Chol molar ratios were prepared. Experimental results showed that as the DOPC/Chol ratio increased, the particle size increased from about 103.0 ± 6.64 nm (*z*-avg ± SD) to 113.5 nm ± 5.76 nm (*z*-avg ± SD) (Figure 1). There was no obvious trend concerning PDI as DOPC/Chol varied from 2.5:1 to 20:1.

Samples were then measured on days 4, 7, and 10 to monitor any changes. It was established that the PDI of the sample should not exceed 0.2 for an acceptable DOPC/Chol molar ratio [24]. Samples with DOPC/Chol molar ratios of 5:1 and 10:1 were not viable as their PDI values were up to 0.307 ± 0.06 and 0.269 ± 0.04, respectively. Samples 2.5:1 and 20:1 had low PDI, sample 2.5:1 had more consistent *z*-avg values (Δ = 2.7 nm) and less consistent peak size values (Δ = 10.5 nm), and sample 20:1 had less consistent *z*-avg values (Δ = 5.9 nm) but more consistent peak size values (Δ = 4.1). After careful consideration, it was determined that the discrepancies between *z*-avg size and peak size consistency did not significantly affect the PDI or particle size. The DOPC/Chol molar ratio of 20:1 was chosen for further investigation because it had good particle size and a low PDI. Furthermore, high concentrations of Chol increase membrane rigidity, which leads to liposomes that are too stable with poor drug release profiles.

3.3 Characterization of MuA-loaded liposome

The chosen DOPC/Chol molar ratio was 20:1, based on results from the previous section, which yielded the optimum particle size and PDI results. The mean *z*-

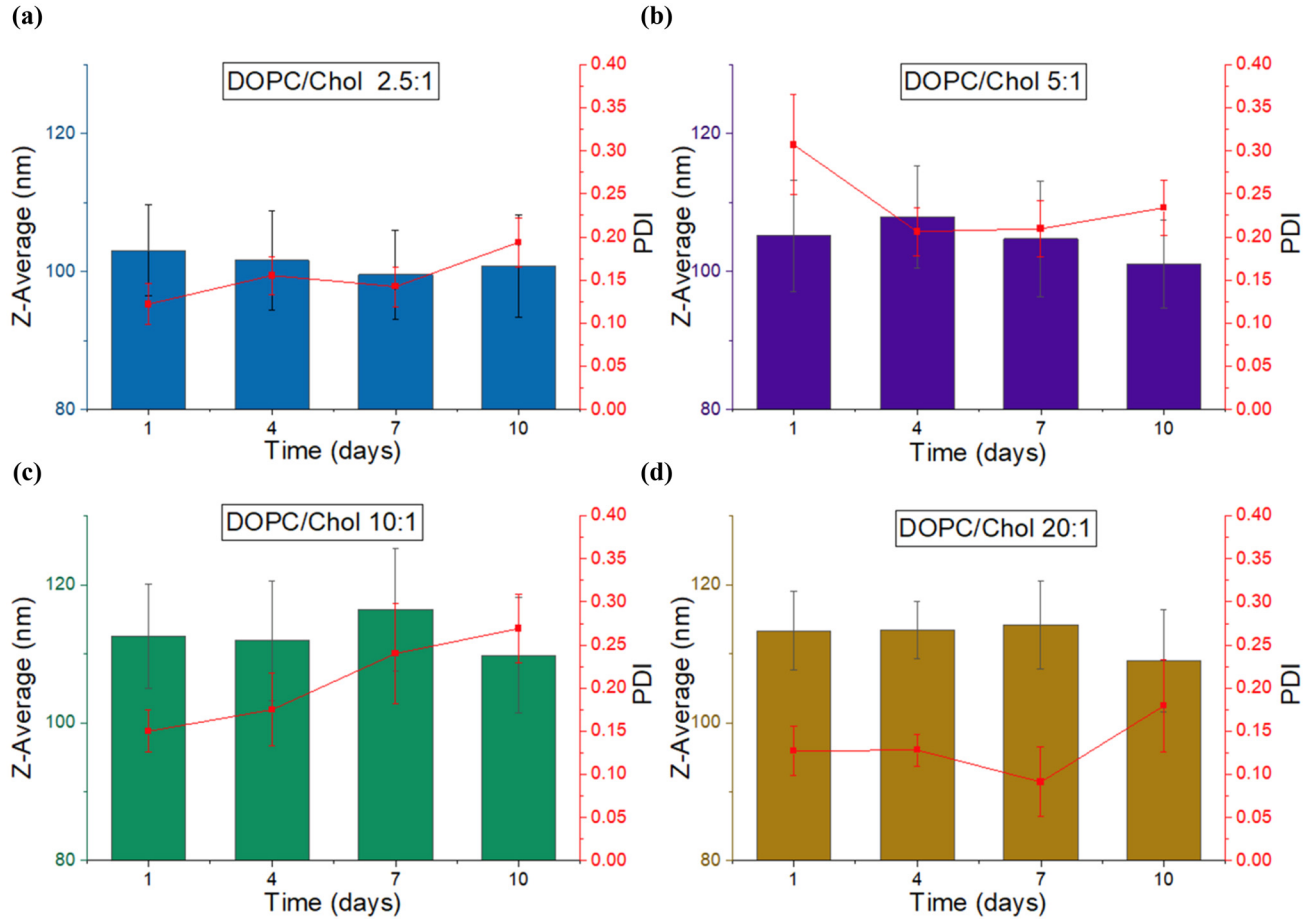

Figure 1: Size distribution of DOPC liposomes with different lipid/Chol ratios. (a) DOPC/Chol ratio 2.5:1 (mol/mol), (b) DOPC/Chol ratio 5:1 (mol/mol), (c) DOPC/Chol ratio 10:1 (mol/mol), and (d) DOPC/Chol ratio 20:1 (mol/mol).

average size of MuA-loaded liposomes was 104.26 ± 6.4 nm (mean ± SD; $n = 3$) before dialysis, with a PDI of 0.15 ± 0.02 (mean ± SD; $n = 3$), as shown in Figure 2. Transmission electron microscopy confirmed that they were of good shape and size, as shown in Figure 2b. The EE% of MuA-loaded liposomes was 55.3 ± 2.3% (mean ± SD; $n = 3$). MuA-loaded liposomes had a particle size of about 100 nm, low PDI, and good EE% (Table 2).

To assess their stability, MuA-loaded liposome samples were kept at 4 or 37°C and measured on days 1, 4, 7, 15, and 30 with DLS. Over a span of 30 days, liposomes stored at 4°C remained stable, with the peak size value shifting from about 105 to 118 m, and relatively narrow peaks (Figure 3a). In contrast, liposomes stored at 37°C began aggregating rapidly after day 7, indicated by significant broadening of the peak corresponding to day 30 (Figure 3b). This could be due to the onset of a heatwave that leads to a spike in temperature (37°C), which resulted in the formation of abnormally large liposomes that skewed the results and much broader intensity distribution peaks. In terms of storage practicality, 4°C is easily attainable by commercial fridges, while freezers can reach as low as −30°C. Further research on the stability of MuA-loaded liposomes over longer time spans (months, years), and the effects of freezing and thawing on MuA-loaded liposome size and distribution will provide more useful information.

The drug release profile of MuA-loaded liposomes is shown in Figure 3c. Free MuA was completely released within 4 h at 37°C or 6 h at 4°C. At 37°C, the drug release profile of MuA-loaded liposomes was biphasic and sustained, obeying linearity from 0 to 6 h to reach around 70% of released MuA, followed by a much longer saturation phase till the end (at 24 h). At 4°C, the release kinetics of MuA-loaded liposome did not show any clear phases and instead increased gradually in a linear manner, reaching 40% released MuA after 24 h. These results implied a correlation between temperature and the release rate. Further research could exploit this property to engineer temperature-sensitive MuA-loaded

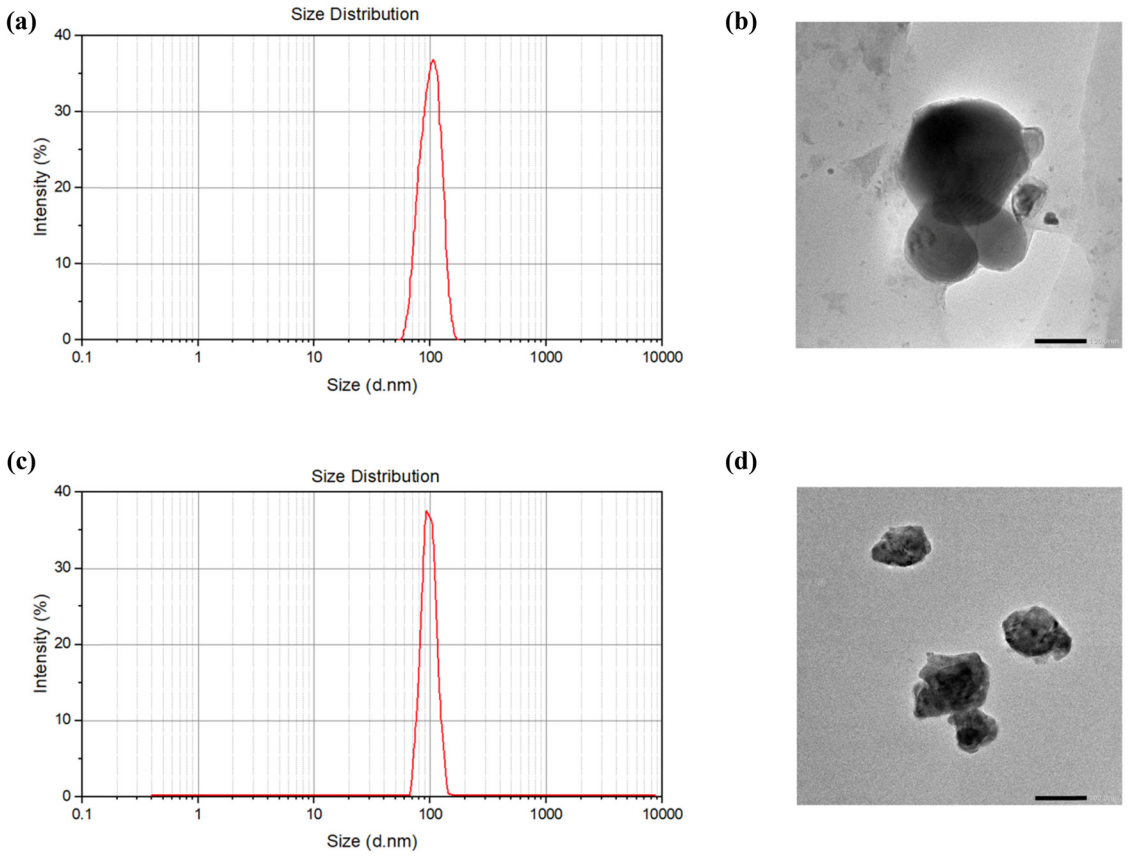

Figure 2: Size distribution of (a) blank liposomes and (c) MuA-loaded liposomes; TEM images of (b) blank liposomes and (d) MuA-loaded liposomes (scale bar 100 nm).

Table 2: The measured physical properties of DOPC/Chol liposomes and MuA-loaded liposomes (n = 3) in PBS (pH 7.4, 0.01 M)

	Particle size (nm)	PDI	Zeta-potential (mV)	EE (%)	DL (%)
DOPC/Chol liposome	113.3 ± 5.76	0.18 ± 0.05	7.50 ± 4.24	—	—
MuA-loaded liposome	104.26 ± 6.4	0.15 ± 0.02	−8.43 ± 5.31	55.32 ± 2.34	8.84 ± 0.16

liposomes, a basic form of targeted delivery. Tumors have been shown to have higher temperatures compared to healthy tissues, possibly due to their higher metabolic rate, or due to their defective vascular architecture, which makes heat exchange by blood less efficient, thereby increasing local temperature. Alternatively, MuA-loaded liposome treatment could be combined with hyperthermia therapy, a cancer treatment that uses heat in the range of 40–45°C to destroy cancer cells and their surrounding blood vessels, or sensitize them to other therapies (e.g., chemotherapy, radiotherapy) [28]. In the case of MuA-loaded liposomes, the elevated tumor temperature induced by hyperthermia therapy could trigger a rapid release of MuA as the liposomes were being absorbed by the cancer cells.

3.4 MTT viability assay

The cytotoxicity of blank liposomes, free MuA, and MuA-loaded liposome were evaluated on HepG2 cells (liver cancer) using the MTT assay (Figure 4). Treatment with blank liposomes did not produce any significant cytotoxic effects, while free MuA and MuA-loaded liposomes induced dose-dependent growth inhibition in HepG2 after 24 h. Compared to free MuA (IC_{50} = 6.24 µg/mL), MuA-loaded liposomes had lower cytotoxicity (IC_{50} = 21.79 µg/mL). This is likely due to the gradual release of MuA from MuA-loaded liposomes compared to the much more rapid release of free MuA. Thus, aside from improving drug solubility, liposomal encapsulation was able to reduce MuA's cytotoxicity.

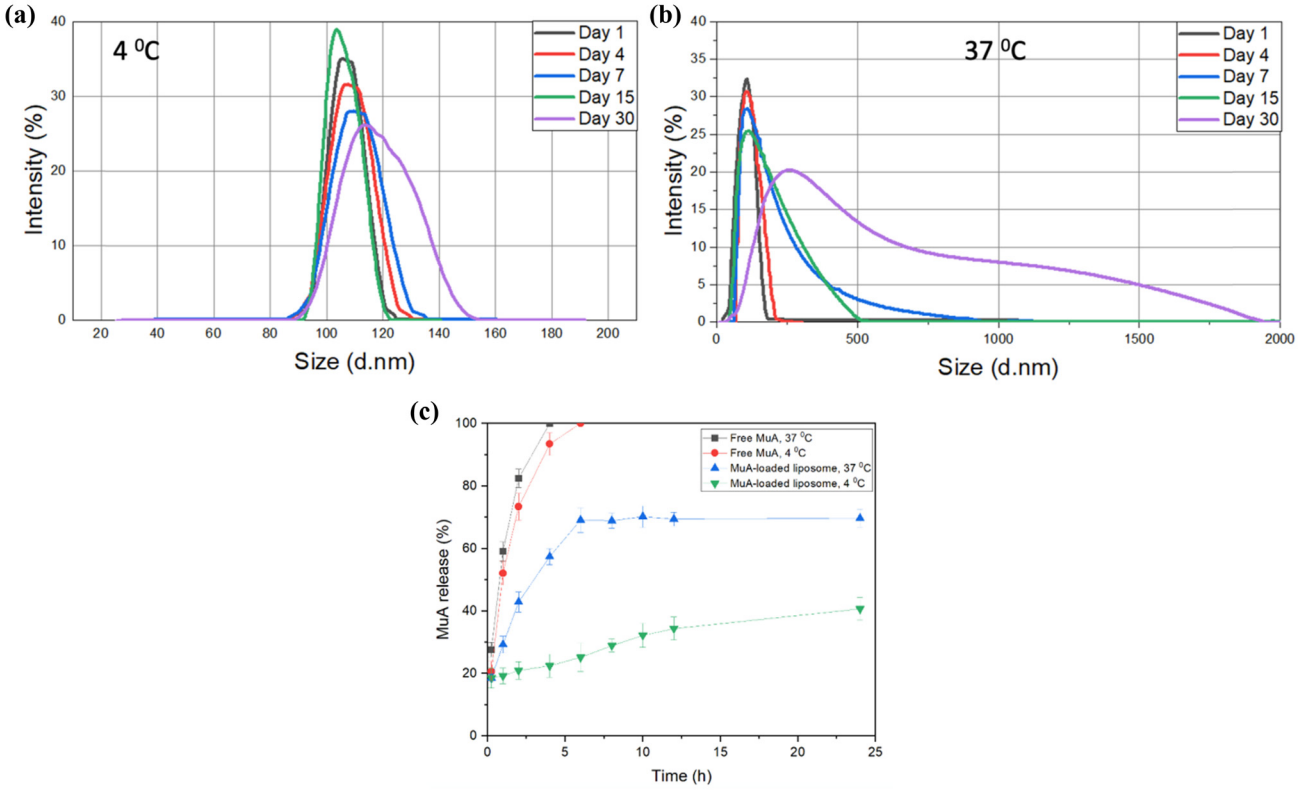

Figure 3: MuA-loaded liposome characterization. (a) Change of liposome size distribution at 4°C and (b) room temperature after 30 days; (c) *in vitro* release profile of free MuA and MuA-loaded liposomes at 4 and 37°C obtained by the dialysis method. Data are presented as mean ± SD (n = 3).

3.5 *In vitro* anti-tumor activity

It has been demonstrated that cell behavior is reflected more accurately in 3D environments compared to 2D environments. A major difference is that 2D cell cultures are exposed to the drug evenly during treatment, which can produce promising results that are misleading. When the same treatment was repeated on 3D cell cultures or *in vivo* models, drug efficiency was lowered. This could be explained by the fact that cancer tumors are composed of multiple cell layers, generating a drug gradient [29]. Thus, cells on the surface are more affected by the drug compared to cells in the core. In our study, HepG2 tumors were grown in PEGDA microwells and incubated at 37°C and 5% CO_2 in humidified air. After day 4, cells began to aggregate and formed cancer spheroids (Figure 5a). Staining with Calcein-AM (green, living) and EthD (red, dead) showed that most of the spheroids was composed of healthy HepG2 cells (Figure 5b).

Cancer spheroids were treated with free MuA, MuA-loaded liposomes, and blank liposomes to test their cytotoxicity. Cell viability was determined with the trypan blue assay, in which dead cells were stained blue. As seen in Figure 6, cell viability decreased at all tested concentrations, indicating that the MuA-loaded liposomes were able to inhibit cell growth in 3D culture.

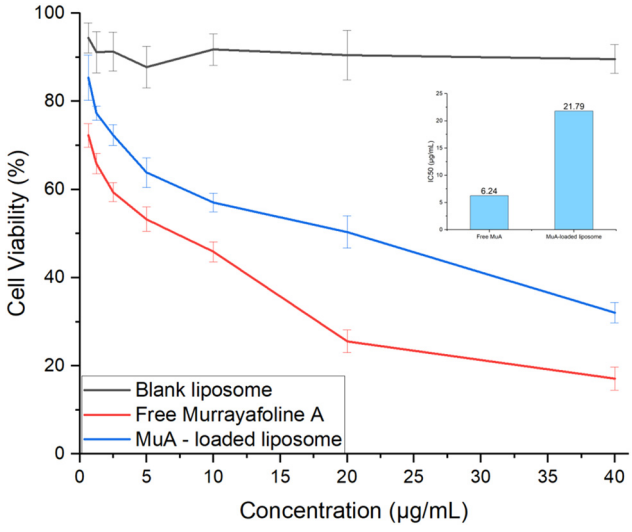

Figure 4: Cytotoxicity of free MuA, blank liposomes, and dialyzed MuA-loaded liposomes against HepG2 cells.

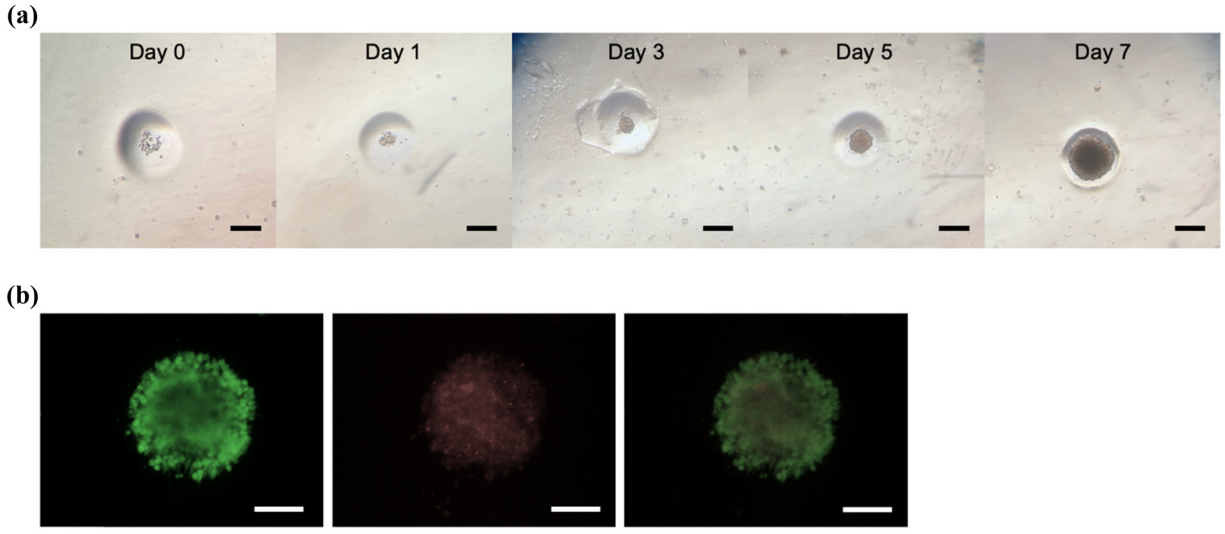

Figure 5: (a) Timeline images of cancer spheroids formation from day 0 to day 7 (scale bar 100 µm), and (b) fluorescence images of cancer spheroid staining with live cells (4 mM Calcein-AM, green), dead cells (2 mM ethidium homodimer-1, red), and merged image of cancer spheroid (scale bar = 100 µm).

Both free MuA and MuA-loaded liposomes were less effective on cancer cells in 3D culture than in 2D monolayer culture. This finding was expected, and is consistent with that of other studies [27]. At the highest tested concentration (50 µg/mL), cell viability was 48% for MuA-loaded liposomes and 30% for free MuA. Although these results implied that MuA-loaded liposomes were less cytotoxic than free MuA even in 3D cultures, the controlled release of MuA-loaded liposomes and improved bioavailability make it a more viable option *in vivo* compared to free MuA. Concerning further research to improve the efficiency of encapsulated MuA, various strategies can be used.

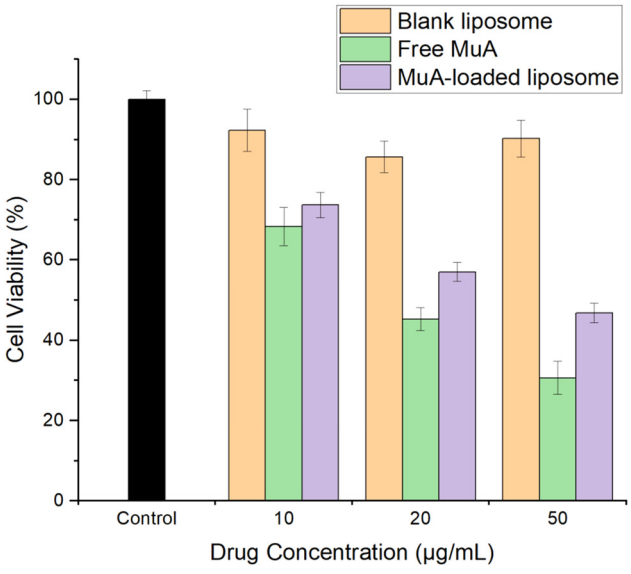

Figure 6: *In vitro* anti-tumor activity of blank liposomes, free MuA, and MuA-loaded liposomes.

A case similar to MuA is of ursolic acid (UA), a natural triterpene compound found in various fruits and vegetables that has been receiving growing interest because of its beneficial effects (e.g., anti-inflammatory, anti-oxidant, anti-apoptotic, anti-carcinogenic). Like MuA, UA's low water solubility leads to poor oral drug absorption in the body, short half-life, and low bioavailability [30]. The addition of PEG to UA-loaded liposomes was able to increase blood circulation time to 48 h, at the cost of no improved anti-tumor activity, possibly due to lowered release rate after PEGylation [31]. Another interesting research direction is pH-sensitive MuA-loaded liposomes, as the pH value of the cancer tumor microenvironment was determined to be more acidic (6.5–7.2 extracellular, 6.0 intracellular lysosome pH) than that of normal tissues (~7.4) [32].

Lopes et al. successfully prepared a type of long-circulating pH-sensitive liposome (SpHL-UA) (average particle size 191.1 nm) that exhibited significant inhibition of MDA-MB-231 cells (breast cancer) (SpHL-UA, IC_{50} 8.13 µM vs free UA, IC_{50} 13.07 µM) [33]. To achieve even higher specificity, encapsulated liposomes can be modified with different ligands, a form of active targeting. A very popular target is the folic acid (FA) receptor because of its significantly higher expression level in many cancer cell types compared to normal tissues, as well as its high affinity for FA molecules [34]. In one study, folate-targeted UA liposomes significantly reduced tumor volume in mice (~55%),

with significantly lower IC_{50} value (22.05 μM) compared to non-targeted (146.3 μM) liposomes [35]. Thus, for future research, MuA liposomes can be PEGylated to increase blood circulation time, and the resulting lowered release rate and cytotoxicity can be offset by the addition of folate ligands to enable active targeting of cancer cells. Additionally, liposome biocompatibility can be improved by using phospholipids from abundant natural sources, such as vegetable oils, egg yolk, and krill [36,37].

4 Conclusion

In this study, the carbazole derivative MuA was extracted from the roots of *G. stenocarpa* at a yield of 0.38% dry root weight. Liposomal formulations at different molar ratios were prepared from the phospholipid DOPC and Chol, and the molar ratio 20:1 (DOPC/Chol) was chosen for further experiments. MuA-loaded liposome formulations were prepared using the thin-film hydration method followed by dialysis and extrusion, and their stability in terms of *z*-average and PDI was evaluated over a span of 30 days. Experimental results demonstrated that the prepared samples had good stability and encapsulation efficiency for drug delivery.

In vitro cytotoxicity of MuA-loaded liposomes against HepG2 cells was evaluated in traditional 2D cell culture with the MTT assay, and in 3D cell culture against tumors grown in PEGDA microwells. The IC_{50} values for 2D and 3D cultures were 21.79 and 43.25 μg/mL, respectively. Compared to the IC_{50} value of MuA in its native form against HepG2 cells, those of MuA-loaded liposomes are lower but safer because they released MuA gradually and theoretically induced less systemic toxicity compared to free MuA. Based on these results, the use of liposomes to encapsulate and deliver MuA is a viable research direction to develop this compound into a more effective chemotherapeutic drug in the future.

Acknowledgments: The authors gratefully acknowledge the support from the Vietnam Academy of Science and Technology.

Funding information: This research was funded by Graduate University of Science and Technology under grant number GUST.STS.ĐT2018-HH02.

Author contributions: Duong Thanh Nguyen devised the main ideas of the project. Dan The Pham, Duong Thanh Nguyen, and Linh Phuong Nguyen wrote the manuscript. Duong Thanh Nguyen, Dan The Pham, and Linh Phuong Nguyen contributed to do experiments and revised the manuscript.

Conflict of interest: The authors declare no conflict of interest.

Ethical approval: The conducted research is not related to either human or animal use.

References

[1] Mohammadian M, Mahdavifar N, Mohammadian-Hafshejani A, Salehiniya H. Liver cancer in the world: epidemiology, incidence, mortality and risk factors. World Cancer Res J. 2018;5(2):1–8.
[2] American Cancer Society AICR. Facts & figures 2019. Am Cancer Soc. 2019;1–76.
[3] Greenwell M, Rahman PK. Medicinal plants: their use in anticancer treatment. Int J Pharm Sci Res. 2015;6(10):4103–12. doi: 10.13040/IJPSR.0975-8232.6(10).4103-12.
[4] Cragg GM, Pezzuto JM. Natural products as a Vital Source for the Discovery of Cancer Chemotherapeutic and Chemopreventive Agents. Med Princ Pract. 2016;25(Suppl 2):41–59. doi: 10.1159/000443404.
[5] Pejin B, Jovanović KK, Mojović M, Savić AG. New and highly potent antitumor natural products from marine-derived fungi: covering the period from 2003 to 2012. Curr Top Med Chem. 2013;13(21):2745–66. doi: 10.2174/15680266113136660197.
[6] Pejin B, Kojic V, Bogdanovic G. An insight into the cytotoxic activity of phytol at in vitro conditions. Nat Prod Res. 2014;28(22):2053–6. doi: 10.1080/14786419.2014.921686.
[7] Mitra S, Sur RK. Hepatoprotection with Glycosmis pentaphylla (Retz). Indian J Exp Biol. 1997;35(12):1306–9.
[8] Silambujanaki P, Bala Tejo Chandra CH, Anil Kumar K, Chitra V. Wound healing activity of Glycosmis arborea leaf extract in rats. J Ethnopharmacol. 2011;134(1):198–201. doi: 10.1016/j.jep.2010.11.046.
[9] Cuong NM, Hung TQ, Van Sung T, Taylor WC. A new dimeric carbazole alkaloid from Glycosmis stenocarpa roots. Chem Pharm Bul. 2004;52(10):1175–8. doi: 10.1248/cpb.52.1175.
[10] Cui CB, Yan SY, Cai B, Yao XS. Carbazole alkaloids as new cell cycle inhibitor and apoptosis inducers from Clausena dunniana Levl. J Asian Nat Prod Res. 2002;4(4):233–41. doi: 10.1080/1028602021000049041.
[11] Kim JH, Yoon J-Y, Kwon SJ, Cho IS, Cuong NM, Choi S-K, et al. Inhibitory components from Glycosmis stenocarpa on pepper mild mottle virus. J Microbiol Biotechnol. 2016;26(12):2138–40.
[12] Han J-H, Kim Y, Jung S-H, Lee J-J, Park H-S, Song G-Y, et al. Murrayafoline a induces a G0/G1-phase arrest in platelet-derived growth factor-stimulated vascular smooth muscle cells. Korean J Physiol Pharmacol. 2015;19(5):421–6. doi: 10.4196/kjpp.2015.19.5.421.

[13] Thuy TTT, Cuong NM, Toan TQ, Thang NN, Tai BH, Nhiem NX, et al. Synthesis of novel derivatives of murrayafoline a and their inhibitory effect on LPS-stimulated production of pro-inflammatory cytokines in bone marrow-derived dendritic cells. Arch Pharm Res. 2013;36(7):832–9. doi: 10.1007/s12272-013-0100-z.
[14] Hu S, Guo J-M, Zhang W-H, Zhang M-M, Liu Y-P, Fu Y-H. Chemical constituents from stems and leaves of Clausena emarginata. Zhongguo Zhong yao za zhi = Zhongguo zhongyao zazhi = China J Chinese Mater Medica. 2019;44(10):2096–101.
[15] Kamil D, Bahadur A, Debnath P, Kumari A, Choudhary SP, Kumar K, et al. First report of stem rot caused by athelia rolfsii on curry leaf tree (Murraya koenigii) in Tripura, India. Plant Dis. 2021;105(2):508. doi: 10.1094/PDIS-05-20-1152-PDN.
[16] Kutz SK, Börger C, Schmidt AW, Knölker HJ. Synthesis of Methylene-Bridged Biscarbazole Alkaloids by using an Ullmann-type Coupling: First Total Synthesis of Murrastifoline-C and Murrafoline-E. Chem Eur J. 2016;22(7):2487–500. doi: 10.1002/chem.201504680.
[17] Cuong NM, Wilhelm H, Porzel A, Arnold N, Wessjohann L. 1-O-Substituted derivatives of murrayafoline A and their antifungal properties. Nat Prod Res. 2008;22(16):1428–32. doi: 10.1080/14786410802006033.
[18] Liu B, Ezeogu L, Zellmer L, Yu B, Xu N, Joshua Liao D. Protecting the normal in order to better kill the cancer. Cancer Med. 2015;4(9):1394–403. doi: 10.1002/cam4.488.
[19] Pérez-Herrero E, Fernández-Medarde A. Advanced targeted therapies in cancer: drug nanocarriers, the future of chemotherapy. Eur J Pharm Biopharm. 2015;93(March):52–79. doi: 10.1016/j.ejpb.2015.03.018.
[20] Shahid N, Erum A, Zaman M, Tulain UR. pH-Responsive nanocomposite based hydrogels for the controlled delivery of ticagrelor; in vitro and in vivo approaches. Int J Nanomedicine. 2021;16:6345.
[21] Bozzuto G, Molinari A. Liposomes as nanomedical devices. Int J Nanomedicine. 2015;10:975–99. doi: 10.2147/IJN.S68861.
[22] Allahou LW, Madani SY, Seifalian A. Investigating the application of liposomes as drug delivery systems for the diagnosis and treatment of cancer. Int J Biomater. 2021:3041969.
[23] Arora S, Singh J. In vitro and in vivo optimization of liposomal nanoparticles based brain targeted Vgf gene therapy. Int J Pharm. 2021;608:121095.
[24] Jain A, Jain A, Parajuli P, Mishra V, Ghoshal G, Singh B, et al. Recent advances in galactose-engineered nanocarriers for the site-specific delivery of siRNA and anticancer drugs. Drug Discov Today. 2018;23(5):960–73.
[25] Tibbitt MW, Anseth KS. Hydrogels as extracellular matrix mimics for 3D cell culture. Biotechnol Bioeng. 2009;103(4):655–63.
[26] Ravi M, Paramesh V, Kaviya SR, Anuradha E, Solomon FDP. 3D cell culture systems: advantages and applications. J Cell Physiol. 2015;230(1):16–26.
[27] Fan Y, Avci NG, Duong NT, Dragomir A, Akay YM, Xu F, et al. Engineering a high-throughput 3-D in vitro glioblastoma model. IEEE J Transl Eng Heal Med. 2015;3:1–8.
[28] Behrouzkia Z, Joveini Z, Keshavarzi B, Eyvazzadeh N, Aghdam RZ. Hyperthermia: how can it be used? Oman Med J. 2016;31(2):89–97. doi: 10.5001/omj.2016.19.
[29] Jensen C, Teng Y. Is it time to start transitioning from 2D to 3D cell culture? Front Mol Biosci. 2020 Mar 6;7:33. doi: 10.3389/fmolb.2020.00033.
[30] Wang L, Yin Q, Liu C, Tang Y, Sun C, Zhuang J. Nanoformulations of ursolic acid: a modern natural anticancer molecule. Front Pharmacol. 2021 Jul 5;12:706121. doi: 10.3389/fphar.2021.706121.
[31] Zhao R, Zheng G, Fan L, Shen Z, Jiang K. Guo Y, et al. Carrier-free nanodrug by co-assembly of chemotherapeutic agent and photosensitizer for cancer imaging and chemo-photo combination therapy. Acta Biomater. 2018;70:197–210. doi: 10.1016/j.actbio.2018.01.028.
[32] Hu Y, Gong X, Zhang J, Chen F, Fu C, Li P, et al. Activated charge-reversal polymeric nano-system: the promising strategy in drug delivery for cancer therapy. Polymers (Basel). 2016 Apr 5;8(4):99. doi: 10.3390/polym8040099.
[33] Lopes SCdA, Novais MVM, Teixeira CS, Sampaio KH, Pereira MT, Miranda LA, et al. Preparation, physicochemical characterization, and cell viability evaluation of long-circulating and pH-sensitive liposomes containing ursolic acid. Biomed Res Int. 2013;2013:467147. doi: 10.1155/2013/467147.
[34] Zhang G, Zhang Z, Yang J. DNA tetrahedron delivery enhances doxorubicin-induced apoptosis of HT-29 colon cancer cells. Nanoscale Res Lett. 2017 Aug 15;12(1):495. doi: 10.1186/s11671-017-2272-9.
[35] Yang G, Yang T, Zhang W, Lu M, Ma X, Xiang G. In vitro and in vivo antitumor effects of folate-targeted ursolic acid stealth liposome. J Agric Food Chem. 2014;62(10):2207–15. doi: 10.1021/jf405675g.
[36] van Hoogevest P, Wendel A. The use of natural and synthetic phospholipids as pharmaceutical excipients. Eur J Lipid Sci Technol. 2014;116(9):1088–107. doi: 10.1002/ejlt.201400219.
[37] Le NTT, Cao VD, Nguyen TNQ, Le TTH, Tran TT, Hoang Thi TT. Soy lecithin-derived liposomal delivery systems: surface modification and current applications. Int J Mol Sci. 2019 Sep 23;20(19):4706. doi: 10.3390/ijms20194706.